7-16-2019

An Index to Better Estimate Tropical Cyclone Intensity Change in the Western North Pacific

Woojeong Lee
Korean Meteorological Administration - South Korea

Sung-Hun Kim
Jeju National University - South Korea; University of Hawaii - Manoa

Pao-Shin Chu
University of Hawaii - Manoa

Il-Ju Moon
Jeju National University - South Korea

Alexander Soloviev
Nova Southeastern University, soloviev@nova.edu

Kim Sunghun (Orcid ID: 0000-0002-3955-0486)

Moon Il-Ju (Orcid ID: 0000-0001-9370-0900)

An index to better estimate tropical cyclone intensity change in the western North Pacific

Woojeong Lee[1], Sung-Hun Kim[2,3], Pao-Shin Chu[3], Il-Ju Moon[2], and Alexander V. Soloviev[4]

[1]National Typhoon Center, Korea Meteorological Administration, Namwon-eup, Seoseong-ro, 810beon-gil 2, Seogwipo, Jeju, 63614, Republic of Korea

[2]Graduate Program in Marine Meteorology/Typhoon Research Center, Jeju National University, 102 Jejudaehak-ro, Jeju, 63243, Republic of Korea

[3]Department of Atmospheric Sciences, School of Ocean and Earth Science and Technology, University of Hawai'i at Manoa, Honolulu, Hawaii

[4]Nova Southeastern University, Halmos College of Natural Sciences and Oceanography, Dania Beach, FL, USA

This article has been accepted for publication and undergone full peer review but has not been through the copyediting, typesetting, pagination and proofreading process which may lead to differences between this version and the Version of Record. Please cite this article as doi: 10.1029/2019GL083273

Corresponding author: Sung-Hun Kim (yah13@hanmail.net)

Key Points:

- The depth-averaged temperature more realistically characterizes ocean response than pre-TC sea surface temperature
- The parameterization of the air-sea exchange process is important in computing the thermodynamic energy budget for TCs
- A revised predictor including two key factors shows significant improvement in the TC intensity change prediction

Abstract

A revised predictor called the net energy gain rate (*NGR*) is suggested by considering wind dependent drag coefficient based on the existing maximum potential intensity theory. A series of wind speed dependent *NGR*, known as *NGR-w,* is calculated based on pre-tropical cyclone (TC) averaged ocean temperatures from the surface down to 120 m (at 10-m intervals) to include the TC-induced vertical mixing for 13 years (2004–2016) in the western North Pacific. It turns out that the NGR_{50}-*w* (*NGR-w* based on temperature averaged over top 50 m) has the highest correlation with 24-h TC intensity change compared with the commonly used sea surface temperature-based intensification potential (*POT*), depth-averaged temperature-based *POT* (POT_{DAT}), and constant drag coefficient in the *NGR*. To demonstrate the effectiveness of the NGR_{50}-*w*, we designed and conducted experiments for training (2004–2014) and testing (2015–2016). The model with the NGR_{50}-*w* shows greater skill than the model with POT_{DAT} or *POT* by reducing prediction errors by about 16%.

1. Introduction

While track prediction of tropical cyclones (TCs) has improved steadily over the last three decades (Rappaport et al., 2012), there has been comparatively little advancement in intensity prediction due to the complicated physical mechanisms involved in internal TC dynamics and their interaction with upper-ocean and atmospheric circulation (Elsberry et al., 2013). It is of utmost importance to accurately predict the rapid intensifying and weakening of TCs at the shorter range (within 24-h) because landfalling TCs can undergo significant and quick intensity changes, which could cause huge economic losses and casualties (Lin et al., 2009). Moreover, landfalling typhoons over the East Asian coast, including China, Japan, Korea, and Taiwan, have shown increased intensity since the late 1970s (Mei and Xie, 2016). Improving rapid intensification (RI) forecasts is one of the highest priorities for TC forecasters among many nations and a central focus area of the National Oceanic and Atmospheric Administration's Hurricane Forecast Improvement Project (Gall et al., 2013).

Numerous attempts have been made to predict the 24-h intensity change, especially for the RI cases, based on a statistical-dynamical model (Kaplan et al., 2010; Rozoff and Kossin, 2011; DeMaria et al., 2012; Gao et al., 2016) as well as numerical modeling perspectives (Chen and Gopalakrishnan, 2014; Tallarpragada and Kieu, 2014). According to recent studies, the statistical-dynamical model still shows more skill at all forecast times compared to dynamical models (DeMaria et al., 2014; Kim et al., 2018). Much effort has gone into improving the TC intensity forecast using new predictors (Kaplan et al., 2015), optimizing predictors (Balaguru et al., 2018; Rozoff and Kossin 2011; Goni et al., 2009), or applying a nonlinear approach (Lin et al., 2017) instead of using the multiple-linear regression method. In other words, finding and utilizing a new predictor that accurately represents TC intensity change holds promise for improving forecast performance in statistical-dynamical models.

In exploring the ocean's role in TC intensity changes, it is important to understand the upper ocean thermal structure (UOTS) because of its interaction with TCs (Shay et al., 2000; Emanuel et al., 2004; Pun et al., 2007; Lin et al., 2008; Wada and Usui, 2007; Goni et al., 2009; Kaplan et al., 2010). To estimate the ocean thermal field accounting for the sea surface cooling effect by TC-induced vertical mixing, Price (2009) suggested the depth-averaged temperature (*DAT*),

$$DAT_d = \frac{1}{d}\int_{-d}^{0} T dz, \quad (1)$$

where *d* is the depth of vertical mixing induced by TCs. *DAT* is a more direct and robust metric of the ocean thermal field reflecting interaction between TCs and the ocean than the widely used tropical cyclone heat potential (TCHP), because the latter may misrepresent oceanic conditions in shallow waters.

Maximum potential intensity (MPI) is widely used to estimate the maximum surface wind speed given atmospheric and oceanic environment (Emanuel, 1988, 1995). Lin et al. (2013) modified *MPI*, which is determined by the thermodynamic conditions of sea surface temperature (*SST*) and the atmospheric environment for steady state TCs (Emanuel 1988; Holland, 1997), and used *DAT* to form a new Ocean Coupling Potential Intensity (*OC_PI*) index

$$OC\_PI^2 = \frac{DAT - T_0}{T_0}\frac{C_k}{C_d}(k^* - k), \quad (2)$$

where T_o is the TC outflow temperature determined by the atmospheric vertical profile, C_k is the enthalpy exchange coefficient, C_d is the drag coefficient, k^* is the saturation enthalpy of the sea surface, and k is the surface enthalpy in the TC environment. It has been shown that *OC_PI* reduces overestimation of maximum intensity relative to *SST*-based *MPI* (Lin et al., 2013). In recent years, *OC_PI* has been frequently used to predict intensity and rapid intensification (Gao et al., 2016; Balaguru et al., 2015).

The air-sea exchange processes control the evolution of TCs (Emanuel, 2003). The TC intensity depends on the coefficients of the transfers of momentum (C_d) and enthalpy (C_k) between the ocean and the atmospheric boundary layer (Ooyama, 1969; Emanuel, 1986). The effects of wind speed-dependent exchange coefficients on TCs have been demonstrated in several previous studies (Braun and Tao, 2000; Jenkins, 2002; Bao et al., 2012; Moon et al., 2007; Nolan et al., 2009a, b; Green and Zhang, 2013), and the parameterizations of C_d were deemed a key determinant of TC intensity simulation. The general consensus is that the C_d increases with wind speed until it reaches approximately 60 kt and does not increase above 70 kt (Powell et al., 2003; Donelan et al., 2004; Jarosz et al., 2007; Bell et al., 2012). However, there are still conflicting results and unresolved issues concerning C_d at very high wind speeds

above 120 kt due to limited observations and experiments (Bell et al., 2012; Rotunno and Emanuel, 1987; Montgomery et al., 2010). At extremely high wind speeds above approximately 120 kt, Soloviev et al. (2014) showed that the C_d increases using the unified waveform and two-phase parameterization schemes, whereas Takagaki et al. (2012) showed the value of C_d approaches to constant based on their laboratory measurements. A proper value of C_d at high wind speeds is important to know because the incidence of categories 4 and 5 storms in the northwest Pacific have increased over the last 37 years (Mei and Xie, 2016).

The objective of this study is to improve intensity prediction, especially in a short temporal range of 24-h. We develop a synoptic predictor for intensity change, a net energy gain rate *(NGR)*, which is based on MPI theory (Emanuel 1988). This predictor is derived from *DAT* and a new parameterization scheme of C_d depending on wind speed. A verification of *NGR* is conducted using a perfect-prognosis based multiple linear regression model for the training and test period. The data and methodology are described in section 2. Section 3 presents an improvement in *NGR* for TC intensity change. Section 4 compares *NGR* with two other comparable new indices suggested by others. Discussion and conclusion are given in section 5.

2. Data and methodology

2.1 TC best-track, atmospheric and oceanic data

In this study, TC statistics over the western North Pacific (WNP) during 2004–2016 are obtained from the best track data archived by the Joint Typhoon Warning Center (JTWC). Statistics for analysis are calculated only for TCs that had a wind speed at or above 34 kt. The *SST* and *DAT* were calculated using the Hybrid Coordinate Ocean Model (HyCOM) Navy Coupled Ocean Data Assimilation (NCODA) nowcast/forecast system data provided by the Naval Research Laboratory (NRL). These oceanic variables were averaged within a radius of 200 km from the storm center using pre-storm conditions (three days before). The *DAT* was calculated at various *d* (10–120 m, at 10 m interval $DAT_{10} - DAT_{120}$; $DAT_{10} - DAT_{120}$) and used to calculate the ocean component of *OC_PI* ($OC\_PI_{10} - OC\_PI_{120}$; hereafter named *OC_PIs*). The *OC_PIs* are calculated based on Emanuel's 'pcmin.m' MATLAB function, which is available online (ftp://texmex.mit.edu/pub/emanuel/TCMAX/pcmin.m). Atmospheric variables were calculated using Global Forecasting System (GFS) analysis data with 1°x1°

spatial and 6-h temporal resolution provided by the National Centers for Environmental Prediction (NCEP).

2.2 The new Net energy Gain Rate

The energy cycle of a mature TC is one of isothermal expansion, adiabatic expansion, isothermal compression, and adiabatic compression (Bister and Emanuel, 1998). Based on Emanuel's *MPI* theory, the energy generation rate (*G)* into the TCs from the sea surface for each square meter of sea surface covered by the storm and the surface frictional dissipation rate (*D*) in the system for each square meter of ocean are given by

$$G = \frac{T_s - T_0}{T_0} C_k \rho V_s (k^* - k), \quad (3)$$

$$D = C_d \rho V_s^3, \quad (4)$$

where C_k is constant value 1.2 $\times$ 10^{-4}, *Ts* is *SST* and V_s is the surface wind speed. The *MPI* is reached at the wind speed where the *G* becomes equal to *D*. Thus, setting *G* equal to *D* and solving for *Vs*, an expression for the maximum possible sustained surface wind speed of a TC is obtained.

$$MPI^2 = \frac{T_s - T_0}{T_0} \frac{C_k}{C_d} (k^* - k) \quad (5)$$

An *NGR* for the western North Pacific basin is developed by incorporating *OC_PI* and wind dependent drag coefficient based on the *MPI* framework. The NGR expresses the realistic response of the sea surface cooling and wave states by TC defined as the difference between DAT based *G* (G_{DAT}) and wind dependent C_d based *D* (D_w) at the "current intensity" resulting from the given thermodynamic environment.

$$NGR = G_{DAT} - D_w = \frac{DAT - T_0}{T_0} C_k \rho V_s (k_0^* - k) - C_{d(V_s)} \rho V_s^3 \quad (6)$$

Larger (smaller) *NGR* implies that the more (less) energy will be used for TC intensification.

Note that while *NGR* is the difference between *G* and *D* at the current intensity, when $G = D$ and therefore $NGR = 0$, the TC reaches a steady state and *MPI* can be derived by solving for Vs. The *NGR* was computed and formulated in two ways to conduct a sensitivity test to evaluate the impact of C_d dependence on wind speed for parameterization of the air-sea exchange process. The first one is a default where C_d is set to be a constant (1.33×10^{-3}) in equation (6) using the 'pcmin.m' program, hereafter referred to as the "traditional set of *NGR* (*NGR-t)*". The second is derived from equation (6) but C_d fitting depending on wind speed is applied instead of the traditionally used constant C_d. For winds below 120 kt, we utilize the unified C_d parameterization scheme interpolated from available field and laboratory data (Soloviev et al., 2014). For winds above 120 kt, C_d is assumed to be constant (2.0×10^{-3}). This will be referred to as the "wind dependency set of *NGR* (*NGR-w)*". The *MPI* is averaged along the track of the storm using the best track data positions at 6-h intervals excluding current forecast time.

3. Results

The intensification potential (*POT*) is defined as the difference between *MPI* and the current intensity. The *POT* is considered the most important predictor in the statistical-dynamical TC intensity prediction models (DeMaria and Kaplan, 1994, 1999; Chen et al., 2011). In particular, *DAT*-based *POT* shows the highest correlation coefficient with intensity change (Kim et al., 2018). We note that, like *POT*, our new predictor *NGR* is also related to the difference between *MPI* and current intensity but the relationship takes a different functional form. Figure 1 presents the correlation coefficients between 24-h TC intensity change and various mixing depths for three groups—*POT*, *NGR-t,* and *NGR-w*—during 2004–2016. Note that the correlation is also carried out for *SST* alone, which is shown at the leftmost margin of the abscissa.

For each individual group, *DAT*-based variables generally exhibit higher correlation coefficients than *SST*-based variables, which are denoted by an open circle in Fig. 1, revealing the importance of using *DAT*. For example, for *SST* based variables the correlation is 0.48 but it reaches as high as 0.64 at DAT_{90} for *NGR-t* (blue curve). For shallow and moderate *DAT* (≤ 60 m), the *NGR-t* has lower correlations than *POT*. The value of constant C_d (0.0013) used to calculate of *NGR-t* is much lower than the observed C_d in the range from 35–63 kt, shown from

previous studies, where probability density of observed TC intensity covers 47.7% of the total (not shown). When constant $C_{d,}$ is used the D for *NGR-t* is underestimated, which results in lower correlation with 24-h TC intensity change than *POT* for $DAT \leq 60$ m. The *DAT*-based *POT* (black curve) correlates significantly with the intensity change at the 1% test level as reported in a previous study (Kim et al., 2018). Note that an even higher correlation coefficient (0.69) is found between the TC intensity change and DAT-based *NGR-w* (red curve). This implies that the dependence of the wind speed on C_d in many studies is important because C_d plays an important role in contributing to the energy budget for TC intensity. Because *NGR-w* using a wind speed dependent C_d represents the TC energy budget more realistically than *NGR-t* using a traditional constant C_d, this new predictor is likely to exhibit the highest correlation to 24-h TC intensity change.

It is somewhat surprising that the correlations between *NGR-w* and intensity change drop dramatically for $DAT \geq 80$. It is well known that the strength of maximum wind speed is the dominant factor in TC-induced vertical mixing and the typical vertical mixing depth for a major TC (category 3 to 5) is about 100 m (Price, 2009). The deep mixing depth (≥ 80 m) based on *DAT* is suited for strong TCs, but can cause underestimation of G in equation (3) for relatively weak TCs. Therefore, the correlation coefficient of deep *DAT* based-*NGR* is lower because the DAT used is too deep (or too cold) for weak TCs and the frequency of strong TC events is very low.

The correlation coefficient of *DAT*-based *POT* for the longer lead times after 42-h tends to be higher than *NGR-w* (Fig. S1). This is due to the use of the TC current intensity when the G and D are calculated in equation (6). Consequently, the TC intensity uncertainty increases with increasing forecast lead time. According to the Fisher's z test (Wilks, 2011), the difference in the correlation coefficient between NGR-w and other predictors is significantly different within 42-h forecast lead times as denoted by the dashed lines in Fig. S1 at the 5% test level (e.g., the p-value is smaller than 0.05). Note that *DAT* based *NGR-w* attains the maximum correlation coefficient with 24-h TC intensity changes at 50 m (Fig. 1). In Fig. 2, we compare the spatial distribution of the composite of 24-h observed TC intensity change, NGR_{50}-*w, POT*, and *POT* at DAT_{50} (POT_{50}) for the period 2004–2016. The areas of observed positive TC intensity changes span the main TC development region (MDR; 5°–20°N, 110°–160°E) in the warm pool of the Philippine Sea and the South China Sea before making landfall or

undergoing extratropical transition (Fig. 2a). The regions of negative TC intensity changes are found from the Yellow Sea extending northeastward through the Kuroshio extension region. The *POT* and POT_{50} have patterns similar to the observations but show TC intensity changes that are too strong throughout the MDR and too weak or rare at higher latitudes (Figs. 2c and 2d). On the other hand, the NGR_{50}-*w* has a distribution closest to the observations in both positive and negative TC intensity change regions (Fig. 2b). The pattern correlations between the observed 24-h TC intensity change and the corresponding *POT*, POT_{50}, and NGR_{50}-*w* are computed over a 1° latitude-longitude box centered at each grid point for the period of 2004–2016. The correlations are 0.66, 0.68, and 0.77 for the aforementioned three predictors, respectively, and the correlation between NGR_{50}-*w* and intensity change is statistically significant at the 1% level (Chu and Zhao, 2007) when Quenouille's (1952) method is used to account for the reduction in the effective number of degrees of freedom due to persistence. This result lends support that the NGR_{50}-*w,* which has the highest pattern correlation coefficient and captures most of the observations for a 24-h TC intensity change. To compare the prediction skill of the main predictors (*POT*, POT_{50}, NGR_{90}-*t* and NGR_{50}-*w*), perfect prognosis-based multiple linear regression models are developed for 24-h intensity change based on a combination of each of the aforementioned main predictors, together with previous 12-h intensity change (PER) and 850–200 hPa vertical wind shear (SHRD). The last two predictors are widely used for intensity prediction and are always included as two additional predictors (Knaff et al., 2005; Kaplan et al., 2015; Gao et al., 2016). As listed in Table 1, four sets of experiments are designed: (1) a run with the use of *POT* (hereafter referred to as the EXP1); (2) a run with the use of DAT_{50}-based POT (POT_{50}) (hereafter referred to as the EXP2); (3) a run with the use of DAT_{90} based *NGR-t* (NGR_{90}-*t*) (hereafter referred to as the EXP3); and (4) an experiment using the NGR_{50}-*w* (hereafter referred to as the EXP4). The four experiments are conducted to predict the 24-h TC intensity change over the WNP during 2004–2016. The SHRD is averaged within a 200 km radius after vortex removal.

The performance of four models in terms of mean absolute error (MAE) and R-squared (coefficient of determination) is estimated from the training (2004–2014) and test (2015–2016) periods. For the training period, MAE and R-squared were compared among the four models. Results show that EXP1 (using *POT*) is comparable to EXP2 (using POT_{50}) and EXP3 (using NGR_{90}-*t*), while EXP4 (using NGR_{50}-*w*) shows the best performance (Table 1). EXP4 explains

the highest R-squared (55%) and has the lowest error (11.42 kt). For the independent period, the NGR_{50}-*w* is, again, the best predictor with the lowest error and highest R-squared among four experiments (Table 1). Relative to EXP1, the 24-h intensity change error decreases by up to 16% when the predictor NGR_{50}-*w* is used. These improvements in the EXP4 for the training (test) period are statistically significant at the 5% (1%) level. Because the NGR_{50}-*w* more realistically characterizes the interaction between TCs and the ocean using C_d depending on wind speed compared with NGR_{90}-*t* that uses a constant C_d, it serves as an effective predictor in improving prediction of TC intensity change at the shorter lead times (within 24-h).

A comparison of the correlation coefficients between 24-h TC intensity change and each of three groups (*POT*, *NGR-t*, and *NGR-w*) are also examined by classifying TCs into seven intensity categories according to initial maximum wind speed: tropical storm (TS; 34–47 kt); severe tropical storm (STS; 48–63 kt); category-1 (CAT1; 64–82 kt); category-2 (CAT2; 83–95 kt); category-3 (CAT3; 96–112 kt); category-4 (CAT4; 113–136 kt); and category-5 (CAT5; above 137 kt). Figure 3a shows the maximum correlation coefficients from *SST* to DAT_{120} for 24-h TC intensity changes for three groups. Figure 3b displays the mixing depth with the highest correlations for the seven TC categories and all three groups. When storms are in the weakest stage (TS), the highest correlations are almost identical for all three groups and occur at a very shallow mixing depth (~10 m) as shown in Fig. 3b. Intense TCs tend to have higher correlations with a deeper *DAT* for all groups and intensity categories. It also appears that the average mixing depth for *NGR-w* is ~50 m (Fig. 3b). As expected, the *NGR-w* exhibits a higher correlation with 24-h TC intensity change than *POT* for intensities below CAT3 (Fig. 3a), while *NGR-w* does not perform as well for the intensities above CAT4. In fact, the *NGR-w* has the lowest correlation coefficient among these three groups, especially for the intensities above CAT5. This implies that constant C_d (2.0×10^{-3}) at extreme winds may not be optimal and one may parameterize C_d with an increasing or a decreasing value or a constant but different value. The behavior of the air-sea exchange coefficient is controversial and still unclear at extreme wind speeds. We will return to this point later.

4. A comparison with predictors from other recent studies

This study also examined the effect of the use of TC-induced mixing depth varying with an individual TC state (T_{dy}). This is motivated by recent studies (Balaguru et al., 2015;

Balaguru et al., 2018) that suggest using T_{dy} yields a better prediction of TC intensification based on the National Hurricane Center's Statistical Hurricane Intensity Prediction Scheme. Following Balaguru et al. (2015) we calculate T_{dy} from the JTWC archive and HyCOM data for the same period and use the wind dependent C_d as applied to *NGR-w* as described in section 2.2 (NGR_T_{dy}). Our results show that NGR_T_{dy} has a lower correlation (r = 0.64) with 24-h TC intensity than NGR_{50}-*w* (r = 0.69), which is contrary to our expectations. However, the difference in correlations between Balaguru et al. (2015, 2018) and our study is not statistically significant.

A possible reason for this result could be the TC-wave-ocean coupling effect on momentum flux. Fan et al. (2009, 2010) showed that momentum flux is significantly reduced because of the strong dependence on the wave-induced processes near the ocean subsurface in a fully coupled wind-wave-ocean model. This reduction can be as large as 25% depending on the choice of the C_d parameterization. The parameterization of TC-induced mixing depth is therefore recommended to include the effect of wave-current interaction. Further studies are needed to find out more realistic drag coefficients when waves are incorporated in the parameterization scheme.

As mentioned previously, the behavior of C_d under very high wind speed conditions is uncertain although the *NGR-w* used here is wind dependent up to 120 kt. It might be possible for C_d to increase (Soloviev et al., 2014) or not change significantly at extreme wind speeds (Bell et al., 2012). It would be interesting to compare the results of *NGR-w* to an *NGR* using an increasing C_d above 120 kt (*NGR-i*). A series of *NGR-i* is calculated (Soloviev et al., 2014) and we find that *NGR-i* also has a high correlation with 24-h TC intensity change for all *DAT*. The maximum correlation coefficient of *NGR-i* is 0.68 at DAT_{50}, which is slightly lower than the NGR_{50}-*w* (r=0.69). Therefore, in cases where C_d at very high wind speed is not known, a constant C_d may be used.

5. Discussion and Conclusion

A statistical-dynamical technique for TC intensity prediction combining statistical methodology with environmental predictors derived from numerical weather prediction system has been widely used over the last 25 years (DeMaria and Kaplan, 1994; DeMaria and Kaplan, 1999; DeMaria et al., 2005). The development of a new predictor, which has a high correlation

with TC intensity, is directly connected to the improvement in prediction skill for a statistical-dynamical model.

The *DAT*-based *POT* shows higher correlation with 24-h intensity change than *SST*-based *POT*. However, for all the *DAT* (10–120 m) including *SST*, *NGR*-*w* has higher correlations than *DAT*-based *POT* (Fig. 1) and improved 24-h TC intensity prediction using NGR_{50}-*w* is achieved during both the training and independent periods (Table 1). The addition of a wind dependent C_d to the dissipation term in *NGR*-*w* thus led to better prediction results for 24-h intensity change. The findings in this study indicate that the best performance in predicting 24-h TC intensity change was by the model at depth of 50 m (DAT_{50}). This is somewhat different from the results of Price (2009) and Lin et al. (2013), who suggested that the best results for the ocean thermal field representing TC-ocean interaction are obtained from DAT_{100} and DAT_{80}, respectively. This difference may be attributed to the fact that all TC cases are used in this study while the two previous studies only focused on stronger TCs.

To improve TC intensity change or rapid intensity change forecasts, this study suggests that *POT* predictors may be replaced by NGR_{50}-*w* because the latter more realistically represents the ocean contribution to 24-h TC intensity change. In addition, the NGR_{50}-*w* can be used to analyze the 24-h TC intensity changes in the currently best-performing intensity prediction models such as the Statistical Hurricane Intensity Prediction Scheme and Statistical-dynamical Typhoon Intensity Prediction Scheme, because both models show little improvement at the shorter ranges (24–48 h) (DeMaria et al., 2014).

Many studies have shown that TC intensity change is closely related to *DAT* and the parameterization of the air-sea exchange processes. We propose *NGR,* a new variant of an intensity change predictor related to Emanuel's MPI that uses the *DAT*, which includes information from TC-induced vertical mixing, and C_d dependent on wind speed (instead of a traditional constant C_d). We show that the new index, NGR_{50}-*w*, improves the hindcasts of 24-h TC intensity change and anticipate that this new index will contribute to improvements in real-time TC intensity forecasts, not only for the western North Pacific but also for other basins.

The NGR_{50}-*w* showed an overall positive bias (Fig. S2) for a steady-state condition. This implies that in addition to frictional dissipation, other environmental factors such as vertical wind shear might be considered with TC intensity changes in real time forecasts. Lin et al. (2013) reported that *OC_PI* is overestimated by about 10–20% because the atmospheric portion of the MPI equation is calculated under the assumption that the atmospheric profile

does not have sufficient time to quickly adjust to the *DAT*. In this study, the *G* is also calculated in the same manner, which results in positive bias of NGR_{50}-*w* for a steady state. In addition, it should be noted that the correlation of NGR_{50}-*w* with intensity change is higher than the other predictors at shorter ranges (within 42-h). Indeed, this result was statistically significant based on the Fisher's z test, at the 5% test level from 6 to 36 h, 6 to 30h and 12 to 42 h compared with the correlation of *POT,* POT_{50}, NGR_{90}-*t,* respectively, while after 48 h the correlation coefficient does not reach 95% significance (Table S1). This is because the value of intensity dependent *NGR* is calculated by the TC current intensity. Therefore, the TC intensity uncertainty increases with increasing forecast lead time and inconsistency between initial wind strength and TC intensities at the forecast lead times also increases.

We showed that the *NGR* index better estimates TC intensity change in the western North Pacific. Future work will apply the *NGR* index to other TC basins and verify that DAT_{50} shows the best performance in predicting 24-h TC intensity change in this study with other years and other basins.

Acknowledgments

This research was supported by the "Research and Development for Numerical Weather Prediction and Earthquake Services in KMA" funded by the National Typhoon Center/Korea Meteorological Administration and basic Science Research Program through the National Research Foundation of Korea (NRK) funded by the Ministry of Education (2017R1A2B2005019). The authors wish to thank May Izumi of the School of Ocean and Earth Science and Technology, University of Hawaii and Luba Solonenko of Nova Southeastern University for their editorial assistance. TC data can be found in JTWC (http://www.metoc.navy.mil/jtwc/jtwc.html?western-pacific), NCEP data at https://nomads.ncdc.noaa.gov/data/gfsanl/, and HyCOM NCODA data at https://www.hycom.org/dataserver/.

References

Balaguru, K., G. R. Foltz, L. R. Leung, E. D′Asaro, K. A. Emanuel, H. Liu, and S. E. Zedler (2015), Dynamic potential intensity: An improved representation of the ocean′s impact on tropical cyclones, *Geophys. Res. Lett.*, *42*, 6739–6746, doi: 10.1002/2015GL064822.

Balaguru, K., G. R. Foltz, L. R. Leung, S. M. Hagos, and D. R. Judi (2018), On the use of ocean dynamic temperature for hurricane intensity forecasting, *Wea. Forecasting, 33,* 411–418, doi: 10.1175/WAF-D-17-0143.1

Bao, J.-W., S. G. Gopalakrishnan, S. A. Michelson, F. D. Marks, and M. T. Montgomery (2012), Impact of physics representations in the HWRFX model on simulated hurricane structure and wind–pressure relationships, *Mon. Wea. Rev., 140*, 3278–3299.

Bell, M. M., M. T. Montgomery, and K. A. Emanuel (2012), Air-sea enthalpy and momentum exchange at major hurricane wind speeds observed during CBLAST, *J. Atmos. Sci*. *69*, 3197–3222.

Bister, M., and K. A. Emanuel (1998), Dissipative heating and hurricane intensity, *Meteor. Atm. Phys*., *52*, 233–240.

Braun, S. A., and W.-K. Tao (2000), Sensitivity of high-resolution simulations of Hurricane Bob (1991) to planetary boundary layer parameterizations*, Mon. Wea. Rev*., *128*, 3941–3961.

Chen, H., and S. Gopalakrishnan (2014), A study on the asymmetric rapid intensification of Hurricane Earl (2010) using the HWRF system. *Proc. 31st Conference on Hurricanes and Tropical Meteorology*. San Diego, CA, 17D.5.

Chen, P., H. Yu, and J. C. L. Chan (2011), A western North Pacific tropical cyclone intensity prediction scheme, *Acta Meteor. Sin., 25*, 611–624, https://doi.org/10.1007/s13351-011-0506-9.

Chu, P.-S., and X. Zhao, 2007: A Bayesian regression approach for predicting tropical cyclone activity over the central North Pacific, *J. Climate, 20*, 4002–4013.

DeMaria, M., and J. Kaplan (1994), A statistical hurricane intensity prediction scheme (SHIPS)

for the Atlantic basin, *Wea. Forecasting, 9*, 209–220.

DeMaria, M., and J. Kaplan (1999), An updated statistical hurricane intensity prediction scheme (SHIPS) for the Atlantic and eastern North Pacific basins, *Wea. Forecasting*, *14*, 326–337.

DeMaria, M., M. Mainelli, L. K. Shay, J. A. Knaff, and J. Kaplan (2005), Further improvements to the Statistical Hurricane Intensity Prediction Scheme (SHIPS), *Wea. Forecasting*, *20*, 531–543.

DeMaria, M., R. T. DeMaria, J. A. Knaff, and D. Molenar (2012), Tropical cyclone lightning and rapid intensity change, *Mon. Wea. Rev.,140*, 1828–1842, doi: 10.1175/MWR-D-11-00236.1.

DeMaria, M., C. R. Sampson, J. A. Knaff, and K. D. Musgrave (2014), Is tropical cyclone intensity guidance improving? *Bull. Amer. Meteorol. Soc.*, *95,* 387–398.

Donelan, M. A., B. K. Haus, N. Reul, W. J. Plant, M. Stianssnie, H. C. Graber, O. B. Brown, and E. S. Saltzman (2004), On the limiting aerodynamic roughness of the ocean in very strong winds, *Geophys. Res. Lett., 31,* L18306, doi: 10.1029/2004GL019460.

Elsberry, R. L., L. Chen, J. Davidson, R. Rogers, Y. Wang, and L. Wu (2013), Advances in understanding and forecasting rapidly changing phenomena in tropical cyclones, *Trop. Cyclone Res. Rev., 2*, 13–24.

Emanuel, K. A. (1986), An air-sea interaction theory for tropical cyclones. Part I: Steady-state maintenance, *J. Atmos. Sci., 43*, 585–604.

Emanuel, K. A. (1988), The maximum intensity of hurricanes, *J. Atmos. Sci., 45*, 1143–1155, doi: 10.1175/1520-0469(1988)045,1143:TMIOH.2.0.CO;2.

Emanuel, K. A. (1995), Sensitivity of tropical cyclones to surface exchange coefficients and a revised steady-state model incorporating eye dynamics*, J. Atmos. Sci., 52*, 3969–3976.

Emanuel, K. A. (2003), A similarity hypothesis for air–sea exchange at extreme wind speeds, *J. Atmos. Sci., 60,* 1420–1428.

Emanuel, K. A., C. DesAutels, C. Holloway, and R. Korty (2004), Environmental control of

tropical cyclone intensity, *J. Atmos. Sci., 61*, 843–858.

Fan, Y., I. Ginis, and T. Hara (2009), The effect of wind-wave-current interaction on air-sea momentum fluxes and ocean response in tropical cyclones, *J. Phys. Oceanogr.*, *39*, 1019–1034.

Fan, Y., I. Ginis, and T. Hara (2010), Momentum flux budget across the air-sea interface under uniform and tropical cyclone winds, *J. Phys. Oceanogr.*, *40*, 2221–2242.

Gall, R., J. Franklin, F. Marks, E. N. Rappaport, and F. Toepfer (2013), The Hurricane Forecast Improvement Project, *Bull. Amer. Meteor. Soc., 94*, 329–343, doi: 10.1175/BAMS-D-12-00071.1.

Gao, S., W. Zhang, J. Liu, I.-I. Lin, L. S. Chiu, and K. Cao (2016), Improvements in typhoon intensity change classification by incorporating an ocean coupling potential intensity index into decision trees, *Wea. Forecasting, 31*, 95–106.

Goni, G., M. DeMaria, J. Knaff, C. Sampson, I. Ginis, F. Bringas, A. Mavume, C. Lauer, I.-I. Lin, P. Sandery, S. Ramos-Buarque, K. Kang, A. Mehra, E. P. Chassignet, and G. Halliwell (2009), Applications of satellite-derived ocean measurements to tropical cyclone intensity forecasting, *Oceanography*, *22(3),* 190–197.

Green, B. W., and E. Zhang (2013), Impacts of air–sea flux parameterizations on the intensity and structure of tropical cyclones, *Mon. Weather Rev. 141*, 2308–2324.

Holland, G. J. (1997), The maximum potential intensity of tropical cyclones, *J. Atmos. Sci., 54*, 2519–2541.

Jarosz, E., D. A. Mitchell, D. W. Wang, and W. J. Teague (2007), Bottom-up determination of air-sea momentum exchange under a major tropical cyclone, *Science, 315*, 1707–1709.

Jenkins, A. D. (2002), Do strong winds blow waves flat?, in *Ocean Wave Measurement and Analysis: Proceedings of the Fourth International Symposium, WAVES 2001: September 2– 6, 2001, San Francisco, California,* edited by B. L. Edge and J. M. Hemsley, pp. 494–500, Am. Soc. of Civ. Eng., Reston, Va.

Kaplan, J., and Coauthors (2015), Evaluating environmental impacts on tropical cyclone rapid

intensification predictability utilizing statistical models, *Wea. Forecasting*, *30,* 1374.1396, https://doi.org/10.1175/WAF-D-15-0032.1.

Kaplan, J., M. DeMaria, and J. A. Knaff (2010), A revised tropical cyclone rapid intensification index for the Atlantic and eastern North Pacific basins, *Wea. Forecasting, 25*, 220–241, doi: 10.1175/2009WAF2222280.1.

Kim, S.-H., I.-J. Moon, and P.-S. Chu (2018), Statistical-dynamic typhoon intensity predictions in the western North Pacific using track pattern clustering and ocean coupling predictors, *Wea. Forecasting, 33*, 347–365.

Knaff, J. A., C. R. Sampson, and M. DeMaria (2005), An operational Statistical Typhoon Intensity Prediction Scheme for the western North Pacific, *Wea. Forecasting*, *20*, 688–699.

Lin, I.-I., C. C. Wu, I. F. Pun, and D. S. Ko (2008), Upper-ocean thermal structure and the western North Pacific category-5 typhoons. Part I: Ocean features and category-5 typhoon's intensification, *Mon. Wea. Rev., 136*, 3288–3306.

Lin, I.-I., C.-H. Chen, I.-F. Pun, W. T. Liu, and C.-C. Wu (2009), Warm ocean anomaly, air sea fluxes, and the rapid intensification of tropical cyclone Nargis (2008), *Geophys. Res. Lett., 36, L03817.*

Lin, I.-I., and coauthors (2013), An ocean coupling potential intensity index for tropical cyclones, *Geophys. Res. Lett*. *40*, 1878–1882.

Lin, N., R. Jing, Y. Wang, E. Yonekura, J. Fan, and L. Xue (2017), A statistical investigation of the dependence of tropical cyclone intensity change on the surrounding environment, *Mon. Wea. Rev., 145,* 2813–2831, https://doi.org/10.1175/MWR-D-16-0368.1.

Mei, W., and S.-P. Xie (2016), Intensification of landfalling typhoons over the northwest Pacific since the late 1970s, *Nature. Geoscience., 9*, 753–757.

Montgomery, M. T., R. K. Smith, and S. V. Nguyen (2010), Sensitivity of tropical-cyclone models to the surface drag coefficient, *Q. J. R. Meteorol. Soc. 136*, 1945–1953, doi: 10.1002/qj.702.

Moon, I.-J., I. Ginis, T. Hara, and B. Thomas (2007), A physics-based parameterization of air–sea momentum flux at high wind speeds and its impact on hurricane intensity predictions, *Mon. Wea. Rev., 135*, 2869–2878.

Nolan, D. S., J. A. Zhang, and D. P. Stern (2009a), Evaluation of planetary boundary layer parameterizations in tropical cyclones by comparison of in situ observations and high-resolution simulations of Hurricane Isabel (2003). Part I: Initialization, maximum winds, and the outer-core boundary layer, *Mon. Wea. Rev., 137*, 3651–3674.

Nolan, D. S, D. P. Stern, and J. A. Zhang (2009b), Evaluation of planetary boundary layer parameterizations in tropical cyclones by comparison of in situ observations and high-resolution simulations of Hurricane Isabel (2003). Part II: Inner-core boundary layer and eyewall structure, *Mon. Wea. Rev., 137*, 3675–3698.

Ooyama, K. (1969), Numerical simulation of the life cycle of tropical cyclones, *J. Atmos. Sci. 26*, 3-40.

Powell, M. D., P. J. Vickery, and T. A. Reinhold (2003), Reduced drag coefficient for high wind speeds in tropical cyclones, *Nature, 422*, 279–283.

Price, J. F. (2009), Metrics of hurricane-ocean interaction: Vertically-integrated or vertically-averaged ocean temperature?, *Ocean Sci., 5*, 351–368.

Pun, I. F., I.-I. Lin, C. R. Wu, D. S. Ko, and W. T. Liu (2007), Validation and application of altimetry-derived upper ocean thermal structure in the Western North Pacific Ocean for typhoon intensity forecast, *IEEE Trans. Geosci. Remote Sens., 45(6)*, 1616–1630.

Quenouille, M. A. (1952), *Associated Measurements*, Butterworths, 242 pp.

Rappaport, E. N., J. G. Jiing, C. W. Landsea, S. T. Murillo, and J. L. Franklin (2012), The joint hurricane testbed—Its first decade of tropical cyclone research-to-operations activities revisited, *Bull. Am. Meteor. Soc., 93*, 371–380.

Rotunno, R., and K. A. Emanuel (1987), An air-sea interaction theory for tropical cyclones. Part II: Evolutionary study using a nonhydrostatic axisymmetric numerical model, *J. Atmos. Sci., 44*, 542–561.

Rozoff, C. M., and J. P. Kossin (2011), New probabilistic forecast models for the prediction of tropical cyclone rapid intensification, *Wea. Forecasting, 26*, 677–689.

Shay, L. K., G. J. Goni, and P. G. Black (2000), Effects of a warm oceanic feature on Hurricane Opal, *Mon. Wea. Rev., 128,* 1366–1383.

Soloviev, A. V., R. Lukas, M. A. Donelan, B. K. Haus, and I. Ginis (2014), The air-sea interface and surface stress under tropical cyclones, *Sci. Rep. 4,* 5306, doi: 10.1038/srep05306.

Soloviev, A. V., R. Lukas, M. A. Donelan, B. K. Haus, and I. Ginis (2017), Is the state of the air-sea interface a factor in rapid intensification and rapid decline of tropical cyclones? *J. Geophys. Res., Oceans*, *122,* doi: 10.1002/2017JC013435.

Takagaki, N., S. Komori, N. Suzuki, K. Iwano, T. Kuramoto, S. Shimada, R. Kurose, and K. Takahashi (2012), Strong correlation between the drag coefficient and the shape of the wind sea spectrum over a broad range of wind speeds, *Geophys. Res. Lett., 39, L23604,* doi.: 10.1029/2012GL053988.

Tallarpragada, V., and C. Kieu (2014), Real-time forecasts of typhoon rapid intensification in the north Western Pacific basin with the NCEP operational HWRF model, *Trop. Cyclone Res. Rev., 3(2),* 63–76.

Wada, A., and N. Usui (2007), Importance of tropical cyclone heat potential for tropical cyclone intensity and intensification in the Western North Pacific, *J. Oceanogr., 63*, 427–447.

Wilks, D. S. (2011), *Statistical Methods in the Atmospheric Sciences*, 3rd ed., Elsevier, 676 pp.

Table 1. Experimental designs for investigating the effect of using the NGR_{50}-*w* on 24-h TC intensity change. The correlation coefficients between the predictors and 24-h TC intensity change during 2004–2016 are indicated in parentheses. The numbers in the subscript of *POT* and *NGR* refer to the depth of the ocean (in meters). The PER and SHRD indicate previous 12-h intensity change and 850–200 hPa vertical wind shear. Mean absolute error (MAE) and R-squared of 24-h TC intensity changes for four experiments are also compared during the training period (2004–2014) and test period (2015–2016).

Experiment	Predictor 1	Predictor 2	Predictor 3	Training period (2004–2014)		Test period (2015–2016)	
				MAE (kt)	R^2	MAE (kt)	R^2
EXP1	*POT* (0.62)	PER (0.39)	SHRD (-0.36)	12.04	0.51	13.18	0.38
EXP2	POT_{50} (0.63)			12.02	0.51	13.07	0.40
EXP3	NGR_{90}-*t* *(0.64)*			12.26	0.48	12.40	0.43
EXP4	NGR_{50}-*w* (0.69)			11.42	0.55	11.33	0.51

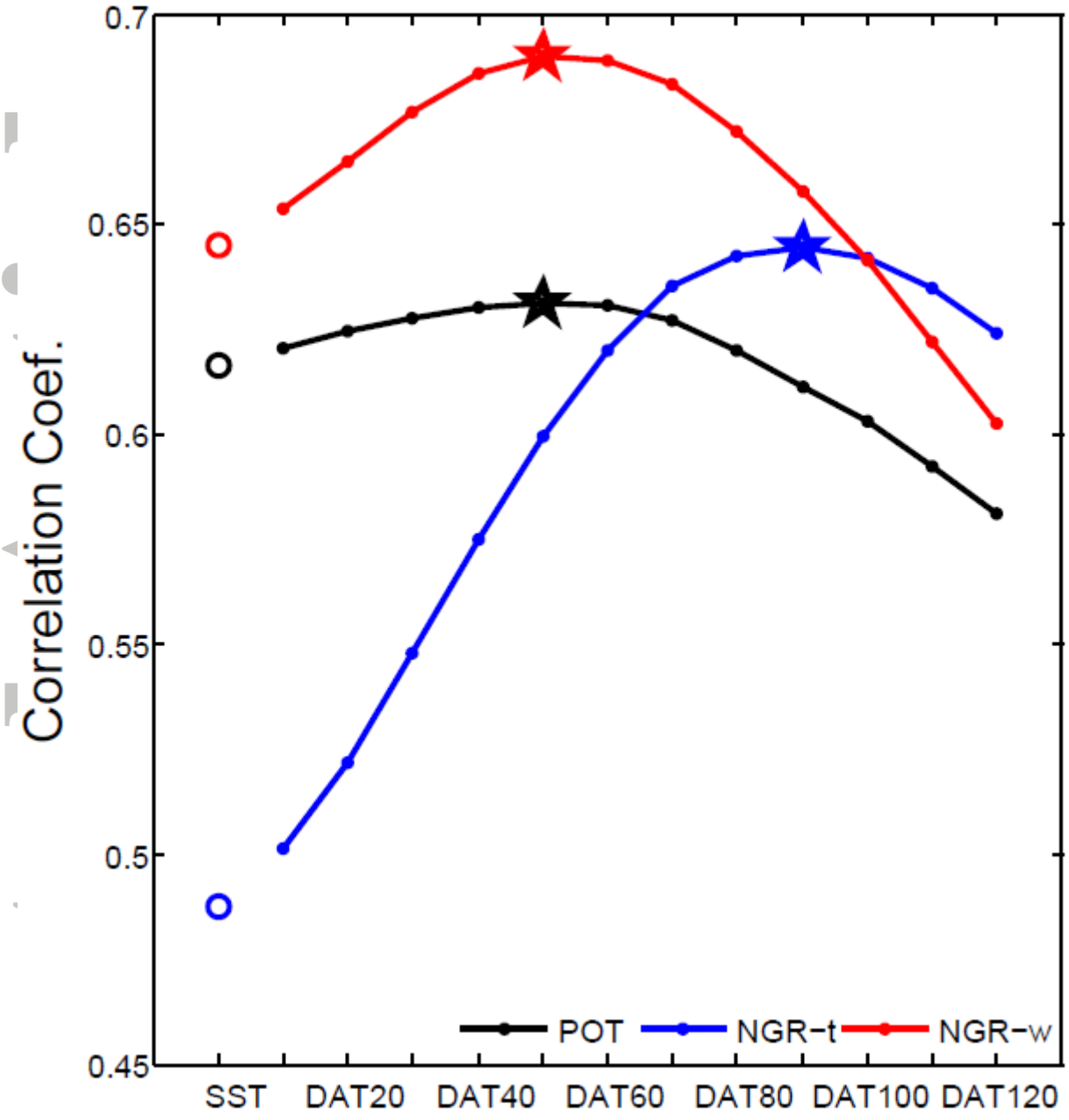

Figure 1. The comparison of the correlation coefficients between a series of *POT*, *NGR-t,* and *NGR-w* from SST to DAT120 by computed ocean temperature averaged over surface to 120 m depth (at 10 m interval) and the 24-h changes in TC intensity during 2004–2016. Pentagrams represent the location of maximum value for each group (*POT*, the intensification potential; *NGR-t*, net energy gain rate using constant drag coefficient; *NGR-w*, same as *NGR-t* but for changing drag coefficient).

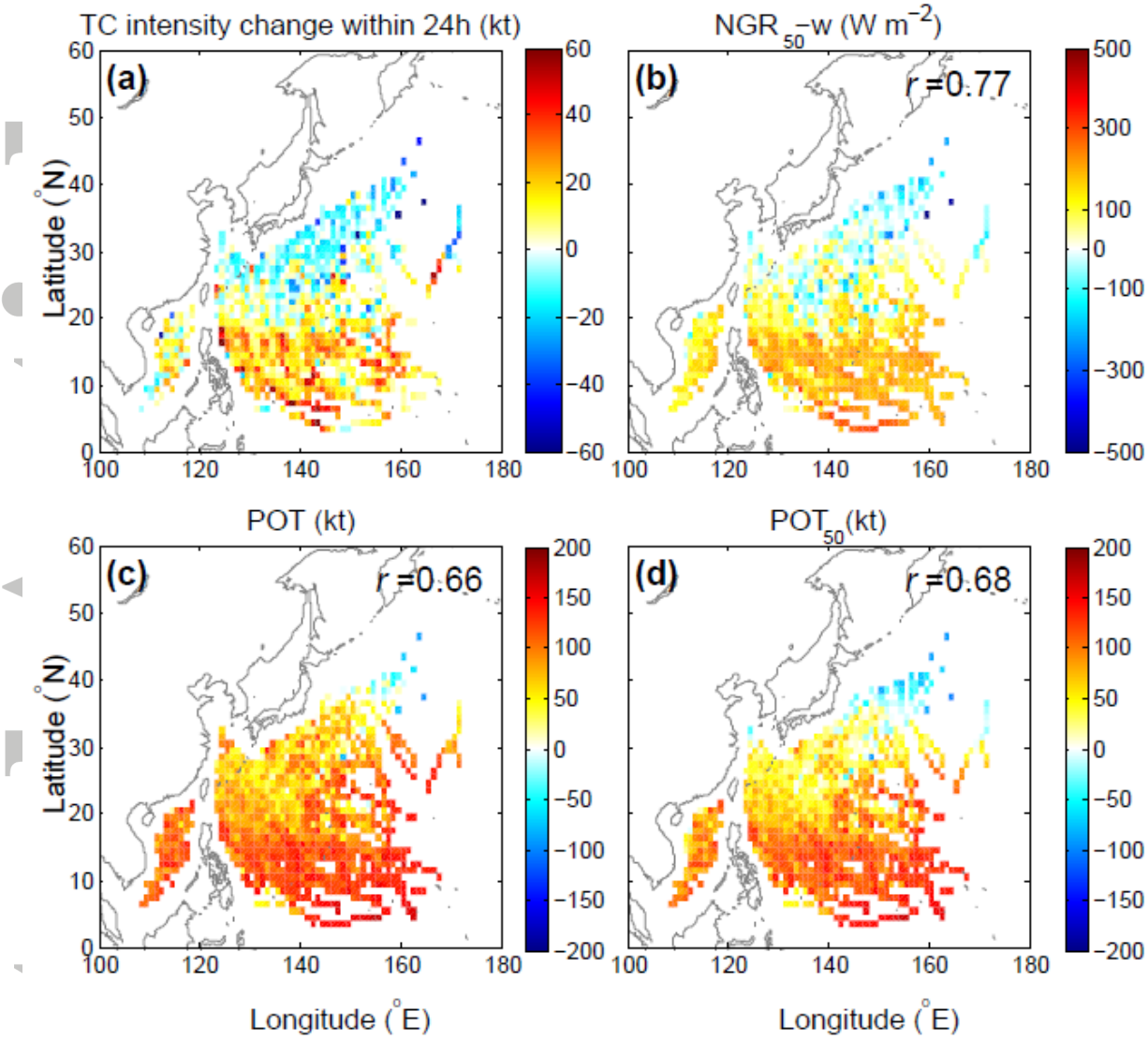

Figure 2. Composite (a) 6-hourly observed 24-h TC intensity change (kt), (b) NGR_{50}-w (Wm^{-2}), (c) POT (kt), and (d) POT_{50} (kt) in the 1°x 1° grid boxes during the period 2004–2016. The numbers in the top-right corner of (b)–(d) panel denote the correlation coefficient with (a).

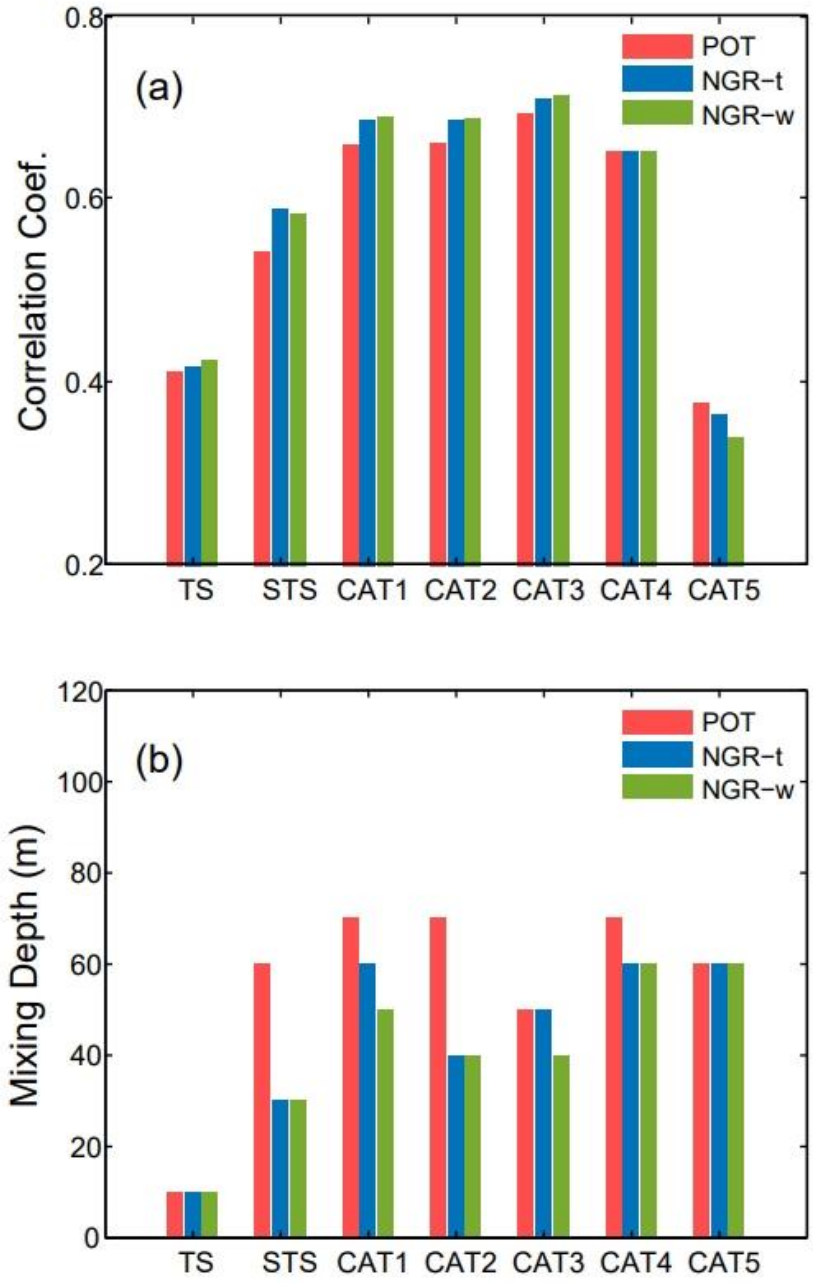

Figure 3. A comparison of the (a) maximum correlation coefficients from *SST* to *DAT*120 between 24-h TC intensity change for three groups and (b) the mixing depth with the highest correlations by classifying TCs into seven intensity categories.